RSC Advances

ROYAL SOCIETY OF CHEMISTRY

www.rsc.org/advances

Journal Name

RSCPublishing

ARTICLE

Delivery of dexamethasone from electrospun PCL-PEO binary fibers and their effects on inflammation regulation

Cite this: DOI: 10.1039/x0xx00000x

Received xxth xx 2014,
Accepted xxth xx 2014

DOI: 10.1039/x0xx00000x

www.rsc.org/

Yan-Fang Li,[a,b] Marina Rubert,[a] Ying Yu,[b] Flemming Besenbacher[a] and Menglin Chen[a]*

Electrospinning of immiscible polymer blends of PCL and PEO has rendered the solid, straight and hydrophobic PCL fibers into porous, hydrophilic microfibers. In this study, electrospun PCL, 11.4%PEO-88.6%PCL and 23.1%PEO-76.9%PCL fibers were loaded with dexamethasone (DEX) without changing the morphology. Their anti-inflammatory properties on Raw 264.7 cells were compared *in vitro*. All fibers were found biocompatible and the encapsulation of DEX could alleviate LPS induced inflammation response. Differences in surface topography, chemical composition, wettability and release kinetics among the different fibers collectively affected the regulation on inflammatory related gene expressions.

Introduction

Despite recent developments in advanced material science, stem cell science and developmental biology, the organisms' innate host inflammatory response to implant biomaterials and medical devices is still a major challenge in tissue engineering. The innate immune response normally helps to eliminate infections, dead tissues, and initiates recovery process. However, it can also lead to persistent tissue damage if targeted destruction and assisted repair are not properly achieved, and an excessive inflammation is detrimental to tissue function.[1-3] Besides, inflammation is a critical component of tumor progression; the inflammatory cells are powerful tumor promoters in the early neoplastic progress.[4] Therefore, it is crucial to maintain the relative balance between the need for inflammation to effectively heal wound and the need to minimize the tissue damage.[5] New functional biomaterials that can regulate the inflammation are still on demand.

The approach of functionalization biomaterial with anti-inflammatory drugs has been proved to effectively modulate the host inflammatory response. Dexamethasone (DEX) is a synthetic glucocorticoid that can regulate the expression of inflammatory cytokines and is clinically used as anti-inflammatory and immunosuppressive drugs.[6-8] Several biomaterials, including microspheres,[9, 10] liposomes,[11] gels[7, 12, 13] and electrospun fibers[6] have been designed to carry DEX and their effective suppression of the inflammation have been proven both *in vivo* and *in vitro*.

Advances in nanotechnology and biotechnology provide opportunities to develop optimal biomaterials to carry anti-inflammatory drugs. Among them, electrospinning is considered to be one of the most promising nanotechnologies. It is a versatile and straightforward technique that can produce continuous sub-micrometer-scale fibers with large surface area, high porosity, controllable mechanical properties, and ease of functionalization.[14-17] Therapeutic molecules such as siRNA,[18, 19] growth factors,[20, 21] and anti-inflammatory drugs [6, 22, 23] can be encapsulated into electrospun fibers directly through mixing in polymer solution for electrospinning.[24, 25] The drug release profile can be tuned by a lot of factors, including fiber morphology, porosity, polymer composition, etc.[26] The fibrous structures of electrospun fibers mimic extracellular matrix; it has been shown that they are biocompatible for a variety of cells,[27-30] and they are good candidates for transplants and medical devices.[31-34] Thus, the electrospun fibers containing anti-inflammatory drugs can regulate the inflammation in the early stages and serve as scaffold for the tissue regeneration in the later stages. Simultaneously, encapsulation of drugs in the electrospun fiber allows localize the drug delivery, providing a more potent effect while eliminating the side-effects associated with systemic administration.

Taking the advantages of drug encapsulated electrospun fibers and their applications in tissue engineering, it is desirable to fabricate anti-inflammatory drug encapsulated into electrospun fibers and study their effects on the regulation of inflammation. Vacanti *et al*[6] studied the effect of electrospun fibers from different polymers on the release kinetics of DEX and on regulation inflammation response. We have previously demonstrated that fiber morphology can be tuned via electrospining of blends of hydrophobic polycaprolactone (PCL) and amphiphilic, protein-adsorption-suppressive polyethylene oxide (PEO).[27] Here, three PCL-PEO blends with intriguingly different morphologies (solid straight fibers, cylinder fibers with holes, and cylinder fibers with lamellar structure) were loaded with DEX directly during the electrospinning. Fiber morphology and composition was evaluated by scanning and transmission electron microscope. The release profile of the DEX was monitored by UV spectroscopy. Macrophage viability was evaluated by determination of lactate dehydrogenase (LDH) activity. The regulation of the inflammation response was evaluated by real-time reverse transcription polymerase chain reaction (RT-PCR). The cell morphology of RAW264.7 cells on PCL electrospun fibers was visualized by confocal microscope.

Experimental

Electrospinning

The PCL/PEO fibers loaded with DEX were fabricated by electrospinning, as previously described by Y-F, Li et al.[27] Briefly, DEX at a concentration of 0.3% (w/w) of the total polymer mass was firstly dissolved in N,N-Dimethylformamide (DMF), then PCL (Mw=70 000-90 000, Sigma-Aldrich) and PEO (Mw=900 000, Sigma-Aldrich) were added to dichloromethane (DCM)/ DMF (3:2) at room temperature and stirring until homogeneous solutions formed. For pure PCL, 20 w/v% PCL was dissolved in DCM/DMF. For the 11.4%PEO-88.6%PCL, 1.8 w/v% PEO and 14 w/v% PCL were dissolved in DCM/DMF. For the 23.1%PEO-76.9%PCL, the ratios of PEO and PCL were changed to 2.4 w/v% and 12 w/v%, respectively. The homogeneous polymer solutions were placed in 1 mL syringe fitted with a metallic needle of 0.9 mm inner diameter. The electrospinning process was carried out under the following conditions: applied voltage=18kV, feeding rate=1 mL/h, distance between the tip of needle and collector=12 cm. The experiments were carried out at room temperature and the relative humidity was between 30%-60%. The obtained fibers were dried under vacuum (labconco Freezone TriadTM) overnight to remove the excess solvents before further use.

Scanning electron microscope

The morphologies of the electrospun fibers were examined with a high-resolution scanning electron microscopy (SEM) (FEI, Nova 600 NanoSEM). The fibers were placed directly into the SEM chamber without any metal sputtering or coating. All the images were captured using secondary electrons detector with an acceleration voltage of 5 kV.

Transmission electron microscope

The internal structure of the fibers was detected by Transmission electron microscopy (TEM) (Tecnai G2 F20 U-TWIN) at 200 kV. All the samples were prepared by electrospinning fibers directly on carbon coated copper grids.

In vitro DEX release

To obtain the release profile of DEX from fibers, fibers were submerged in 10 mL of phosphate buffered saline (PBS) and keep at 37 °C and in humidified conditions for up to 24 hours. At designed time intervals, 500 µL of the solutions were collected and refreshed with equal volume of PBS buffer. To determine the amount of DEX released, sample absorbance's was measured at 242 nm by a UV-Vis spectrophotometer (UV-1800, Shimazu). The concentration of DEX was read off from the linear standard curve, and the percentage of cumulative drug released was then calculated based on the initial weight of DEX incorporated in the fibers.

Cell culture of RAW 264.7 cells on the fibers

The murine RAW 264.7 macrophage-like cell line (ATCC, Manassas, USA) were routinely cultured in DMEM-Glutamax (4,5g L-D-glucose, (-) piruvate) (GIBCO, Grand Island, NY) supplemented with 10% FBS (Biowhittaker, Walkersvile, MD) and antibiotics (100 IU and 100 IU streptomycin antibiotics (Gibco, Grand Island, NY) at 37 ºC in a humidified atmosphere of 5% CO_2. Cells were routinely subcultured 1:10 before reaching confluence by scrapping. All experiments were performed after 17 passages of the RAW 264.7 cells.

Before seeding, the fibers were punched out into circular pieces of the diameter of 12 mm and placed on the bottom of a sterile standard 48-well plate, and a Ø12 mm PCL ring was placed on the top of fibers to keep fibers well on the bottom. Raw 264.7 cells were seeded onto each fiber at a density of 1.6 $*10^5$ cells /cm^2 either with or without treatment with 0.1 µg/ml LPS (LPS, E. Coli 055:B5, Schnelldorf, Germany). In parallel, cells seeded on 48-well tissue culture plate (TCP) and TCP plus 0.1µg/ml lipopolysaccharide (TCP+LPS) served as a negative and positive control, respectively. PCL rings were also placed into the TCP wells, which served as control groups to eliminate the effects of the PCL rings. Cells were maintained in standard cell culture conditions (37°C in a humidified atmosphere of 5% CO_2) for 24 hours.

After 24 hours of cell seeding, culture media was collected to evaluate cytotoxicity (LDH activity). Cell attachment and morphology onto the fibers was also visualized by SEM and confocal microscope. In parallel, expression of marker genes related to inflammation was assessed by real-time RT-PCR. To ensure that the cell characterization was done only on the cells growing onto the fibers, samples were moved to a tube prior gene expression analysis.

Cell viability (Lactate dehydrogenase (LDH) activity)

After 24 hours of cell seeding, the LDH activity in the collected culture media was taken as an indicator of membrane leakage/cell lysis. The activity of the cytosolic enzyme was estimated according to the manufacturer's kit instructions (Roche Diagnostics, Mannheim, Germany) by assessing the rate of oxidation of NADH at 490nm in presence of piruvate. After removing the background from the absorbances of the culture media without cells, results from all the samples were presented relative to the LDH activity in the medium of cells treated cultured on tissue culture plastic (TCP) (low control, 0% of cell death) and of cells cultured on TCP treated with 1% Triton X-100 (high control, 100% cell death). The percentage of LDH activity was calculated using the following equation:
Cytotoxicity (%) = ((exp.value – low control)/ (high control – low control)) * 100.

Total RNA isolation and gene expression of inflammation markers by real-time RT-PCR

The effect of different type of fibers to induce an inflammation response was further studied by quantification of relative mRNA levels of selected inflammation related markers after 24 hours of cell seeding.
Total RNA was isolated from cells using Trizol reagent (Invitrogen Life Technologies, Carlsbad, CA, USA) according to the manufacturer's protocol. Total RNA was quantified at 260 nm using a Nanodrop spectrophotometer (IMPLE AH Diagnostics, Helsinki, Finland). 0.4 µg RNA was reverse transcribed to cDNA at 37 ºC for 60 min using High Capacity RNA-to-cDNA kit (Applied Biosystems, Foster City, CA), according to the protocol of the supplier. Aliquots of each cDNA were frozen (-20 °C) until the PCR reactions were carried out.
Real-time PCR was performed in the Lightcycler 480® (Roche Diagnostics, Mannheim, Germany) using SYBR green detection. Real time RT-PCR was done for three reference genes (18S rRNA, glyceraldehyde-3-phosphate dehydrogenase (GAPDH) and TBP) and 2 target genes (interleukin 1 beta (IL-1β) and nitric oxide synthase (iNOS). The primer sequences were as follows: 18s rRNA-F: 5'-GTAACCCGTTGAACCCCATT -3'; 18s rRNA-R: 5'-CCATCCAATCGGTAGTAGCG -3'; GAPDH-F:5'-ACCCAGAAGACTGTG-GATGG -3'; GAPDH-R: 5'-CACATTGGG-GGTAGGAACAC -3'; TBP-F: 5' -AGAGAGCCACGGACAACTG -3'; TBP-R:5'-ACTCTAGCATATTTTCTTGCTGCT -3'; ILβ-F: 5'-GCCACCTTTTGACAGTGATGA -3'; ILβ-R: 5'-GATGTGCTGCTGCGAGATTT -3'; iNOS-R:5'-GCCACCAACAATGGCAACAT -3'; iNOS-F: 5'-TCGATGCACAACTGGGTGAA -3'.
Each reaction contained 7 µL Lightcycler 480 SYBR GREEN I Master (containing Fast Start Taq polymerase, reaction buffer, dNTPs mix, SYBRGreen I dye and $MgCl_2$), 0.5 µM of each, the sense and the antisense specific primers and 3µl of the cDNA dilution in a final volume of 10 µl. The amplification program consisted of a pre-incubation step for denaturation of the template cDNA (10 min 95 °C), followed by 45 cycles consisting of a denaturation step (10 s 95 °C), an annealing step (10 s 60 °C) and an extension step (10 s 72 °C). After each cycle, fluorescence was measured at 72 °C (λ_{ex} 470 nm, λ_{em} 530 nm). A negative control without cDNA template was run in each assay.
Real-time efficiencies were calculated from the given slopes in the LightCycler 480 software using serial dilutions, showing all the investigated transcripts high real-time PCR efficiency rates, and high linearity when different concentrations are used. PCR products were subjected to a melting curve analysis on the LightCycler and subsequently 2% agarose/TBE gel electrophoresis to confirm amplification specificity, Tm and amplicon size, respectively.
Relative quantification after PCR was calculated by dividing the concentration of the target gene in each sample by the mean of the concentration of the three reference genes (housekeeping genes) in the same sample using the Advanced relative quantification method provided by the LightCycler 480 analysis software version 1.5 (Roche Diagnostics, Mannheim, Germany).

Cell morphology

Cell morphology after 24 hours of seeding was visualized by confocal microscope (CLSM 700 Zeiss, Jena, Germany) . RAW 264.7 cells adhered to the fibers were fixed with 4% formaldehyde in PBS for 15 minutes. For staining, cells were permeabilized in 0.2% triton in phosphate buffered saline (PBS) (Sigma, Schnelldorf, Gemany). The cytoskeleton of the cells was stained using 50µg/ml phalloidin Atto 488 (Sigma Aldrich, Schnelldorf, Germany) and the nuclei with Prolong® Gold Antifade Reagent with DAPI (Invitrogen, Carlsbad, CA, USA).

Statistical analysis

Cytotoxicity and gene expression data were presented as mean values ± standard error of the mean (SEM). Differences between groups were assessed by Mann-Whitney test. The SPSS® program for Windows (Chicago, IL), version 17.0 was used. Results were considered statistically significant at the p-values < 0.05.

Results and discussions

Fiber morphology

The small amount of DEX (0.3% w/w) didn't affect the morphology of the electrospun fibers, compared to fibers without DEX[27] (**Figure 1**). The PCL-DEX fibers were straight solid fibers (**Figure 1a, d**), with the diameter 0.92 ± 0.61 µm. The 11.4%PEO-88.6%PCL-DEX fibers became cylindrical coiled fibers (**Figure 1b**) with abundant pores distributed not only on the surface, but also through the fibers (**Figure 1 e**). The diameter of the fibers was 3.253 ± 0.609 µm. The 23.1%PEO-76.9%PCL-DEX fibers had ultraporous interweaving morphology, which were composed of interconnected lamellae, and the pores were interior within the fibers (**Figure 1c, f**). The diameter of the fibers was 4.782 ± 0.37 µm.

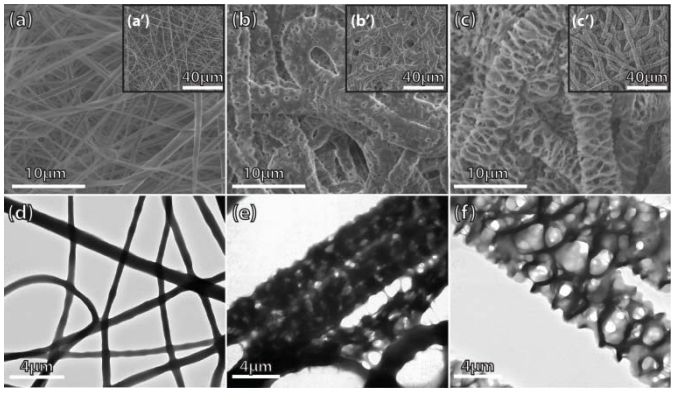

Figure 1. SEM images of electrospining fibers loaded with DEX (a) and (a'): 20%PCL-DEX; (b) and (b'): 11.4%PEO-88.6%PCL-DEX; and (c) and (c') 23.1%PEO-76.9%PCL-DEX. And the lower panel is the TEM images corresponding to the samples in the upper panel.

DEX release

It has been shown that dosages of DEX between $1*10^{-4}$ M and $1*10^{-6}$ M showed highest down-regulation of several inflammation related marker genes with minimal toxicity for the cells.[35] Therefore, DEX at $1*10^{-4}$ M was chosen as the final concentration when 100% DEX was released from the fibers. The release profile of DEX from the electrospun PCL/PEO fibers was shown in **Figure 2**. The PCL-DEX fibers demonstrated an initial release of 35.7% in the first 4 hours followed by a slow and sustained release of 9.0% in the next 20 hours. Whereas, both 11.4%PEO-88.6%PCL-DEX and 23.1%PEO-76.9%PCL-DEX fibers performed significant burst release of DEX of 92.8% and 81.7%, respectively, during the first 4 hours.

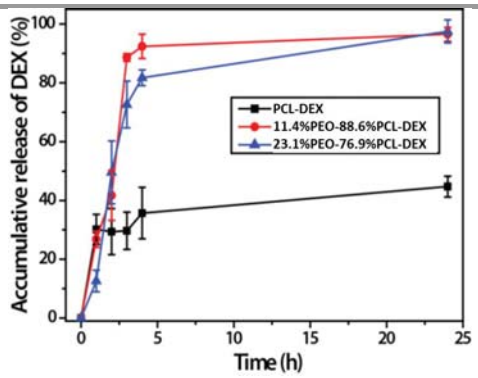

Figure 2. Accumulative release of dexamethasone from the fibers in PBS. Error bars indicate mean ± SD. (n=6 for each time point)

The kinetics of drug release depends on the morphology, porosity, and composition of the matrix, the amount and hydrophilicity of drugs, etc.[26, 36] Due to slow wetting and degradation properties of PCL, the sustained DEX release observed in the PCL-DEX fiber mainly depends on the diffusion. On the contrary, for the 11.4%PEO-88.6%PCL-DEX and 23.1%PEO-76.9%PCL-DEX fibers, which were composed of interconnecting pores and hydrophilic PEO, there was faster wetting; consequently the hydrophilic DEX was quickly released.

Biocompatibility

Raw 264.7 macrophages were seeded on the different groups of DEX-loaded fibers to evaluate their anti-inflammatory properties. Since the fibers were to be applied as implantation scaffolds, the premise is that they must be non-cytotoxic. The effects of DEX-loaded fibers on the viability of cells were firstly investigated by determination of the LDH activity. As shown in **Figure 3**, all of the three DEX-loaded fibers were found biocompatible. Furthermore, each fibers containing DEX significantly decreased the cell toxicity compared to the fibers without DEX respectively, suggesting that the incorporation of DEX improves cell viability and thus the biocompatibility of the fibers. DEX is a glucocorticoid with an important role in the attenuation of the inflammatory response. It has been suggested that glucocortocoids exert their anti-inflammatory action eith inducing death of inflammatory cells or by protecting the resident cells of inflamed tissues by arresting apoptotic signals.[37] In agreement, Raw 264.7 cells cultured on DEX contained fibers thus showed increased viability.

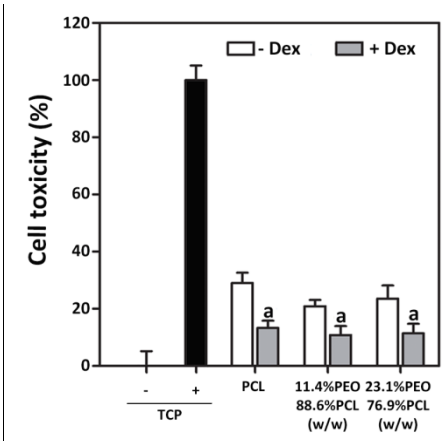

Figure 3. LDH activity measured from culture media collected after seeding Raw 264.7 cells on PCL, 11.4%PEO-88.6%PCL and 23.1%PEO-76.9%PCL with or without containing DEX (10^{-4} M) for 24 hours. High control (100% cytotoxicity) was cell culture media collected form cells seeded on tissue culture plate (TCP) that treated with 1% Triton X-100, and low control (0% cytotoxicity) was cell culture media from cells seeded on TCP. Cell culture media collected form cells cultured on TCP treated by LPS was also measured to evaluate the cytotoxicity of LPS. Error bars indicate mean ± SEM.

Effect of PCL-PEO-DEX fibers on IL1β and iNOS gene expression

It has been previously reported that PCL, 11.4%PEO-88.6%PCL and 23.1%PEO-76.9%PCL are biocompatible and with low inflammation potential upon incubation with macrophages cells.[27] Here we investigated the effect of DEX contained PCL-PEO fibers on regulation of pro-inflammatory cytokines (IL1β) and mediators (iNOS) and whether the different PCL-PEO fibers could affect the DEX effect.

LPS is a prototypical endotoxin formed by phosphoglycolipid which can directly activate macrophage cells.[38] LPS-induced

macrophages increase the production of inflammatory cytokines such as IL-1β, granulocyte/macrophage colony stimulating factors (GM-CSF), and nitric oxide.[39, 40]

Compared to the positive control of inflammation which were Raw 264.7 cells treated with LPS on TCP (TCP+LPS), the macrophages cultured on the DEX-loaded fibers showed significant down-regulations on the inflammatory markers.(**Figure 4**) 11.4%PEO-88.6%PCL-DEX and 23.1%PEO-76.9%PCL-DEX decreased significantly the expression of both IL1β and iNOS, compared to negative control of inflammation (TCP). Interestingly, iNOS mRNA levels decreased along the decrease of PEO content, showing PCL-DEX a significant reduction of 12.7-fold on the expression of iNOS compared to 23.1%PEO-76.9%PCL-DEX. Although PCL-DEX didn't differentiate from negative control (TCP) on the IL1β expression, it markedly decreased the expression of iNOS, with a 27.9 fold (p=0.046) compared to negative control (TCP).

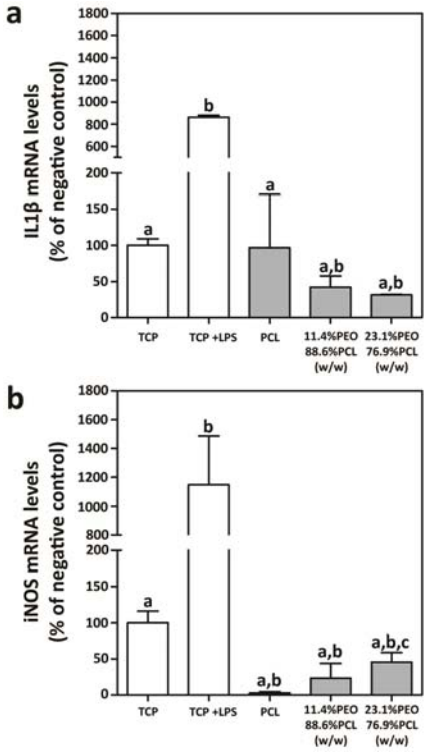

Figure 4. Expression of inflammation related genes after culture of Raw 264.7 macrophage cells on PCL-DEX, PEO11.4%-PCL88.6-DEX, and 23.1%PEO-76.9%PCL-DEX for 24 h. Data represent relative mRNA levels of target genes normalized with reference genes, expressed as a percentage of negative control of inflammation (TCP) cells, which was set to 100%. Differences between groups were assessed by Mann-Whitney test p<0.05: (a) versus positive control of inflammation (TCP +LPS); (b) versus negative control of inflammation (TCP); (c) versus 20%PCL.

Effect of encapsulated DEX on IL1β and iNOS gene expression in LPS-induced macrophages

To further examine whether DEX encapsulated into PCL-PEO fibers are able to diminish the inflammatory response, the gene regulatory effects of the three different fibers on LPS-induced inflamed macrophages cells were evaluated and compared after 24 hours of culture.(**Figure 5)**

The LPS treatment induced up-regulation of inflammatory markers, as seen in **Figure 5**; and the DEX encapsulation down-regulated significantly their expressions.[39, 40] Indeed, DEX significantly decreased the expression of IL1β expression in all the DEX contained fibers to the same level as cells cultured on negative control TCP.(**Figure 5a**)

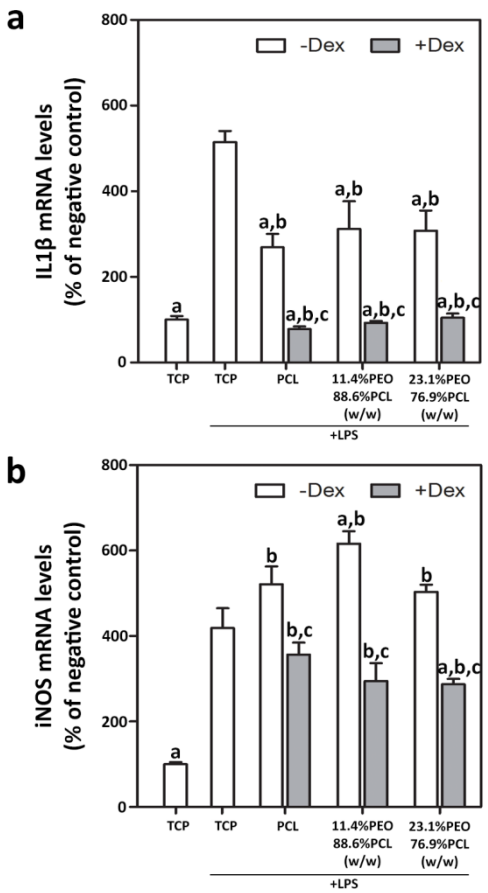

Figure 5. Expression of inflammation related genes after culture of LPS-induced Raw 264.7 macrophage cells on PCL, 11.4%PEO-88.6%PCLand 23.1%PEO-76.9%PCL with or without containing DEX (10^{-4} M) for 24 h. Cells seeded on TCP with or without LPS treatment, serve as negative and positive reference groups of inflammation. Data represent relative mRNA levels of target genes normalized with reference genes, expressed as a percentage of negative control of inflammation (TCP) cells, which was set to 100%. Differences between groups were assessed by Mann-Whitney test p<0.05: (a) versus positive control of inflammation (TCP +LPS); (b) versus negative control of inflammation (TCP); (c) versus each control fiber.

On the other hand, the iNOS level were significantly up-regulated by LPS, even compared to the positive contr TCP+LPS, especially on 11.4%PEO-88.6%PCLfibers with a 1.43 fold increase (p=0.005). Consequently, the expression of iNOS after significant down-regulation by DEX encapsulatio was not significantly different from the positive control TCP+LPS, except that on 23.1%PEO-76.9%PCL-DEX, where a decrease in 1.5 fold (p=0.035) was observed compared o TCP+LPS.(**Figure 5b**)

Therefore, the encapsulated DEX was capable of controlling the acute inflammatory response by decreasing the cell inflammation response. Although the larger diameter of the PCL-PEO fibers could up-regulate the inflammatory responses, the PEO composition might alleviate the responses, together with the higher burst release of anti-inflammatory drug DEX, compared to the PCL fibers. Collectively, there is no difference in the DEX down-regulation potential on LPS-induced macrophages among the PCL-PEO-DEX fibers.

Effect of encapsulated DEX on macrophages morphology

The cell function correlates with their morphological response. As seen under confocal microscopy LPS induced RAW264.7 cells cultured on the fibers containing DEX displayed mainly the more rounded shape as (**Figure 6f-h**) characteristic of non-inflamed macrophages (**Figure 6e**), compare to the cells on the fibers without DEX (**Figure 6b-d**), indicating DEX could alleviate the activation from LPS.

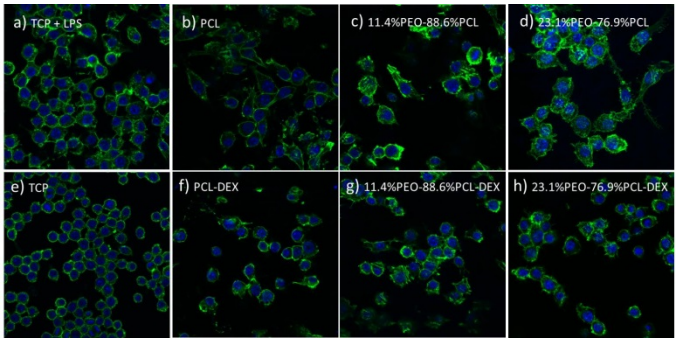

Figure 6. Confocal images of LPS-stimulated RAW 264.7 cells cultured on fibers (a) TCP +LPS, (b) PCL, (c) 11.4%PEO-88.6%PCL, (d) 23.1%PEO-76.9%PCL, (e) TCP, (f) PCL-DEX, (g) 11.4%PEO-88.6%PCL-DEX, and (h) 23.1%PEO-76.9%PCL-DEX.

Conclusions

Electrospinning of immiscible polymer blends of PCL and PEO has rendered the solid, straight and hydrophobic PCL fibers into porous, hydrophilic microfibers. In this study, DEX was encapusulated in the electrospun PCL, 11.4%PEO-88.6%PCLand 23.1%PEO-76.9%PCLfibers without changing their morphologies. The release of DEX was found highly dependent on the wettability of the fibers, where hydrophobic PCL-DEX has less burst release compared to hydrophilic PCL-PEO fibers. All fibers were found biocompatible and the encapsulation of DEX could alleviate LPS induced inflammation response. Differences in surface topography, chemical composition, wettability and release kinetics among the different PCL-PEO-DEX fibers collectively affected the regulation on inflammatory related gene expressions.

Acknowledgements

We gratefully acknowledge the Danish Council for Strategic Research for the funding to the ElectroMed Project at the iNANO Center, and the Aarhus University Research Foundation and the Carlsberg Foundation for their financial support. Yan-Fang Li and Marina Rubert contributed equally.

Notes and references

[a]Interdisciplinary Nanoscience Center (iNANO), Aarhus University, DK-8000 Aarhus C, Denmark. E-mail: menglin@inano.au.dk
[b]Institute of Nanoscience and Nanotechnology, Central China Normal University, Wuhan 430079, China.

References

1. C. Nathan, *Nature*, 2002, **420**, 846-852.
2. S. L. Robbins, V. Kumar, A. K. Abbas and J. C. Aster, *Robbins basic pathology*, Elsevier Health Sciences, 2012.
3. R. Medzhitov, *Cell*, 2010, **140**, 771-776.
4. L. M. Coussens and Z. Werb, *Nature*, 2002, **420**, 860-867.
5. T. A. Butterfield, T. M. Best and M. A. Merrick, *Journal of athletic training*, 2006, **41**, 457.
6. N. M. Vacanti, H. Cheng, P. S. Hill, J. D. T. Guerreiro, T. T. Dang, M. Ma, S. Watson, N. S. Hwang, R. Langer and D. G. Anderson, *Biomacromolecules*, 2012, **13**, 3031-3038.
7. M. J. Webber, J. B. Matson, V. K. Tamboli and S. I. Stupp, *Biomaterials*, 2012, **33**, 6823-6832.
8. D.-H. Kim and D. C. Martin, *Biomaterials*, 2006, **27**, 3031-3037.
9. B. S. Zolnik and D. J. Burgess, *Journal of controlled release*, 2008, **127**, 137-145.
10. T. Hickey, D. Kreutzer, D. Burgess and F. Moussy, *Journal of biomedical materials research*, 2002, **61**, 180-187.
11. U. Bhardwaj and D. J. Burgess, *International journal of pharmaceutics*, 2010, **388**, 181-189.
12. Q. Wang, J. Wang, Q. Lu, M. S. Detamore and C. Berkland, *Biomaterials*, 2010, **31**, 4980-4986.
13. T. Ito, I. P. Fraser, Y. Yeo, C. B. Highley, E. Bellas and D. S. Kohane, *Biomaterials*, 2007, **28**, 1778-1786.
14. N. Bhardwaj and S. C. Kundu, *Biotechnology Advances*, 2010, **28**, 325-347.
15. D. Li and Y. Xia, *Advanced Materials*, 2004, **16**, 1151-1170.
16. J. Doshi and D. H. Reneker, Industry Applications Society Annual Meeting, 1993., Conference Record of the 1993 IEEE, 1993.
17. Z.-M. Huang, Y.-Z. Zhang, M. Kotaki and S. Ramakrishna, *Composites science and technology*, 2003, **63**, 2223-2253.
18. H. Cao, X. Jiang, C. Chai and S. Y. Chew, *Journal of controlled release*, 2010, **144**, 203-212.
19. M. Chen, S. Gao, M. Dong, J. Song, C. Yang, K. A. Howard, J. Kjems and F. Besenbacher, *ACS Nano*, 2012, **6**, 4835-4844.
20. Z. Man, L. Yin, Z. Shao, X. Zhang, X. Hu, J. Zhu, L. Dai, H. Huang, L. Yuan, C. Zhou, H. Chen and Y. Ao, *Biomaterials*, 2014, **35**, 5250-5260.
21. S. Sahoo, L. T. Ang, J. C.-H. Goh and S.-L. Toh, *Journal of Biomedical Materials Research Part A*, 2010, **93A**, 1539-1550.
22. E.-R. Kenawy, F. I. Abdel-Hay, M. H. El-Newehy and G. E. Wnek, *Materials Chemistry and Physics*, 2009, **113**, 296-302.
23. V. Holan, M. Chudickova, P. Trosan, E. Svobodova, M. Krulova, S. Kubinova, E. Sykova, J. Sirc, J. Michalek, M. Juklickova, M. Munzarova and A. Zajicova, *Journal of controlled release*, 2011, **156**, 406-412.
24. M. Chen, Y.-F. Li and F. Besenbacher, *Advanced Healthcare Materials*, 2014, n/a-n/a.

25. S. Chew, Y. Wen, Y. Dzenis and K. Leong, *Current pharmaceutical design*, 2006, **12**, 4751.
26. A. Martins, A. R. C. Duarte, S. Faria, A. P. Marques, R. L. Reis and N. M. Neves, *Biomaterials*, 2010, **31**, 5875-5885.
27. Y.-F. Li, M. Rubert, H. Aslan, Y. Yu, K. A. Howard, M. Dong, F. Besenbacher and M. Chen, *Nanoscale*, 2014, **6**, 3392-3402.
28. P. Sangsanoh, S. Waleetorncheepsawat, O. Suwantong, P. Wutticharoenmongkol, O. Weeranantanapan, B. Chuenjitbuntaworn, P. Cheepsunthorn, P. Pavasant and P. Supaphol, *Biomacromolecules*, 2007, **8**, 1587-1594.
29. S. D. McCullen, D. R. Stevens, W. A. Roberts, L. I. Clarke, S. H. Bernacki, R. E. Gorga and E. G. Loboa, *International journal of nanomedicine*, 2007, **2**, 253.
30. A. S. Badami, M. R. Kreke, M. S. Thompson, J. S. Riffle and A. S. Goldstein, *Biomaterials*, 2006, **27**, 596-606.
31. C. Del Gaudio, A. Bianco and M. Grigioni, *Annali dell'Istituto superiore di sanita*, 2007, **44**, 178-186.
32. J. Stitzel, J. Liu, S. J. Lee, M. Komura, J. Berry, S. Soker, G. Lim, M. Van Dyke, R. Czerw, J. J. Yoo and A. Atala, *Biomaterials*, 2006, **27**, 1088-1094.
33. L. Susan, L. Bojun, M. Zuwei, W. He, C. Casey and R. Seeram, *Biomedical Materials*, 2006, **1**, R45.
34. J. Venugopal and S. Ramakrishna, *Appl Biochem Biotechnol*, 2005, **125**, 147-157.
35. M. Rubert, Y.-F. Li, J. Dehli, M. B. Taskin, F. Besenbacher and M. Chen, *RSC Advances*, 2014, **4**, 51537-51543.
36. H. K. Makadia and S. J. Siegel, *Polymers*, 2011, **3**, 1377-1397.
37. C.-C. Fong, Y. Zhang, Q. Zhang, C.-H. Tzang, W.-F. Fong, R.S.S. Wu, M. Yang, *Toxicology*, 2007, **236**, 16–28.
38. E. T. Rietschel, T. Kirikae, F. U. Schade, U. Mamat, G. Schmidt, H. Loppnow, A. J. Ulmer, U. Zähringer, U. Seydel and F. Di Padova, *The FASEB Journal*, 1994, **8**, 217-225.
39. H. G. Kim, B. Shrestha, S. Y. Lim, D. H. Yoon, W. C. Chang, D.-J. Shin, S. K. Han, S. M. Park, J. H. Park and H. I. Park, *European journal of pharmacology*, 2006, **545**, 192-199.
40. M. Huo, X. Cui, J. Xue, G. Chi, R. Gao, X. Deng, S. Guan, J. Wei, L. W. Soromou and H. Feng, *Journal of Surgical Research*, 2013, **180**, e47-e54.